



# Kinematics estimation of straddled movements on high bar from a limited number of skin markers using a chain model

Mickael Begon, Pierre-Brice Wieber, Maurice Raymond Yeadon

## ► To cite this version:

Mickael Begon, Pierre-Brice Wieber, Maurice Raymond Yeadon. Kinematics estimation of straddled movements on high bar from a limited number of skin markers using a chain model. *Journal of Biomechanics*, 2008, 41 (3), pp.581-586. 10.1016/j.jbiomech.2007.10.005 . inria-00390475

**HAL Id: inria-00390475**

**<https://inria.hal.science/inria-00390475>**

Submitted on 2 Jun 2009

**HAL** is a multi-disciplinary open access archive for the deposit and dissemination of scientific research documents, whether they are published or not. The documents may come from teaching and research institutions in France or abroad, or from public or private research centers.

L'archive ouverte pluridisciplinaire **HAL**, est destinée au dépôt et à la diffusion de documents scientifiques de niveau recherche, publiés ou non, émanant des établissements d'enseignement et de recherche français ou étrangers, des laboratoires publics ou privés.

# Kinematics estimation of straddled movements on high bar from a limited number of skin markers using a chain model

Mickaël Begon <sup>a,\*</sup>, Pierre-Brice Wieber <sup>b</sup>,

Maurice Raymond Yeadon <sup>a</sup>

*<sup>a</sup>School of Sport and Exercise Sciences, Loughborough University*

*Loughborough Leics. LE11 3TU*

*United Kingdom*

*<sup>b</sup>INRIA Rhône-Alpes, Inovallée 655 avenue de l'Europe, Montbonnot 38 334 Saint*

*Ismier Cedex France*

Revision 1 with minor corrections.

Address for correspondence: Dr M. Begon

School of Sport and Exercise Sciences

Loughborough University

Ashby Road – Loughborough

Leicestershire LE11 3TU

United Kingdom

---

## 1 Abstract

2 To reduce the effects of skin movement artefacts and apparent joint dislocations  
3 in the kinematics of whole body movement derived from marker locations, global  
4 optimisation procedures with a chain model have been developed. These procedures  
5 can also be used to reduce the number of markers when self-occlusions are hard  
6 to avoid. This paper assesses the kinematics precision of three marker sets: 16,  
7 11 and 7 markers, for movements on high bar with straddled piked posture. A  
8 three-dimensional person-specific chain model was defined with 9 parameters and  
9 12 degrees of freedom and an iterative procedure optimised the gymnast posture for  
10 each frame of the three marker sets. The time histories of joint angles obtained from  
11 the reduced marker sets were compared with those from the 16 marker set by means  
12 of a root mean square difference measure. Occlusions of medial markers fixed on the  
13 lower limb occurred when the legs were together and the pelvis markers disappeared  
14 primarily during the piked posture. Despite these occlusions, reconstruction was  
15 possible with 16, 11 and 7 markers. The time histories of joint angles were similar;  
16 the main differences were for the thigh mediolateral rotation and the knee flexion  
17 because the knee was close to full extension. When five markers were removed, the  
18 average angles difference was about  $3^\circ$ . This difference increased to  $9^\circ$  for the seven  
19 marker set. It is concluded that kinematics of sports movement can be reconstructed  
20 using a chain model and a global optimisation procedure for a reduced number of  
21 markers.

22 *Key words:* kinematics, chain model, gymnastics, optimisation

---

---

\* Corresponding author.

*Email address:* M.Begon@lboro.ac.uk (Mickaël Begon).

# Kinematics estimation of straddled movements on high bar from a limited number of skin markers using a chain model

## 1 Introduction

In sports biomechanics, as in clinical gait analysis, optoelectronic motion capture systems based on passive markers are widely used to recover human movement descriptors. The poses (position and orientation) of the body segments are determined from skin-mounted markers before their kinematics and kinetics are calculated. In the direct approach (Kadaba et al., 1990), at least three markers per segment are needed for the definition of a segment-embedded reference frame which represents the pose of the segment. This approach has numerous limitations associated with the number of markers and the use of a rigid segment representation. Moreover the kinematics remains inaccurate because no compensation is made for the skin movement artefacts (Reinschmidt et al., 1997a).

The kinematics accuracy can be improved by increasing the number of markers per segment (Challis, 1995). The calculation of the rotation matrices from five markers seems to be a good compromise to limit the damaging effect of skin movement artefacts. In clinical analysis, there exist marker sets (Davis et al., 1991) which are used to minimize the number of markers. Joint centres are defined from static data acquisitions or from measurements on the participant. These marker sets are based on assumptions which allow the medial markers to be removed during walking trials. For these marker sets, the joint centre location is estimated with a predictive approach based on anthropometrical

47 measurement or the midpoint of two markers.

48 Human kinetics calculation is often based on multibody dynamics assuming  
49 pin joints without translation. However with at least three markers, each body  
50 segment can be considered independently of the proximal one and will have  
51 three degrees of freedom (*DoF*) in rotation and three *DoF* in translation.  
52 Kinematic and kinetic parameters are calculated from non-rigid arrays of  
53 markers and procedures have been developed to limit the array deformation  
54 (Chèze et al., 1995; Spoor and Veldpaus, 1980). In these formulations, each  
55 segment is treated independently without guaranteeing a constant segment  
56 length. To reduce skin movement artefacts and apparent joint dislocations, Lu  
57 and O'Connor (1999) proposed a global optimisation procedure with a chain  
58 model. This method has been applied to computer simulated movements of  
59 the lower limbs (Lu and O'Connor, 1999) and the upper limbs (Roux et al.,  
60 2002). Other chain models associated with optimisation procedures have been  
61 used to analyse gait (Charlton et al., 2004; Reinbolt et al., 2005). In Reinbolt  
62 et al. (2005) the determination of the kinematics was based on a two-level  
63 optimisation and required three markers per segment. Performance measures  
64 of this algorithm were estimated for 12-*DoF* synthetic motions.

65 In contrast with gait analysis, no standard marker set can be used satisfactorily  
66 for data collection in sport. Each movement has its own segment deformations  
67 arising from muscle contractions and joint motions together with its own self-  
68 occlusions that require a specific marker set. Additionally, the use of three or  
69 more markers per segment is impractical for whole body sports movements  
70 because of increased marker occlusion, increased soft tissue movement and  
71 increased marker detachment during dynamic movements.

Usually the joints are modelled as ball-and-socket (*e.g.* hip joint or glenohumeral joint) or as hinge joints (*e.g.* knee). If the joint centre location is known then there is some redundancy in using three markers since two will suffice for a three *DoF* joint and one marker will suffice for a single *DoF* joint. The purpose of this study was to determine the kinematics of a movement from a limited number of markers and the definition of a person-specific chain model.

## 2 Methods

A 9-parameter, 3-dimensional, 12-*DoF* model was used to describe the kinematics of circling movements with a piked and straddled posture on the high bar in gymnastics. This chain model was designed for this specific application, but the method allows any model to be defined. Twenty-two technical and anatomical reflective markers were used to define the chain model. Kinematics was calculated from 16, 11 and 7 markers and then the three sets were compared to quantify the effect of the marker number. The model implementation and the kinematics optimisation from real data were performed using the *HuMANs* toolbox under Scilab (Wieber et al., 2006).

The body was considered as an articulated system composed of rigid bodies corresponding to the following segments: upper limbs, scapular girdle, torso-head, pelvis, right thigh, left thigh, right shank-foot and left shank-foot. The kinematics of the left and right lower-limbs was viewed as being symmetrical. Six parameters ( $p_i$ ) and 12 *DoF* ( $q_i$ ) described the chain model (Fig. 1). Flexion, abduction and lateral rotation were defined to be positive and the angle sequence was flexion-extension, abduction-adduction and mediolateral

96 rotation.

97 [Fig. 1 about here.]

98 The participant, a member of the Great Britain Men's Senior Gymnastics  
99 Squad (17 years, 61.6 kg, 1.705 m), gave informed consent to perform a number  
100 of straddled stalders and endos on the high bar (Fig. 2) changing technique  
101 and velocity from trial to trial. Ten successful trials of each of the two circling  
102 movements were selected for analysis.

103 [Fig. 2 about here.]

104 All trials were captured using 18 Vicon cameras operating at 100 Hz and  
105 positioned on a hemisphere on the left side of the subject. A volume centred  
106 on the high bar spanning  $3\text{ m} \times 5\text{ m} \times 5\text{ m}$  was wand calibrated. Twenty-  
107 one spherical markers of 25 mm diameter were attached to the trunk and  
108 the left upper and lower limbs: lateral and medial malleolus ( $T_{1,2}$ ), tibia ( $T_3$ ),  
109 lateral and medial knee ( $T_{4,5}$ ), lateral side of the mid-thigh ( $T_6$ ), left and  
110 right anterior superior iliac spines ( $T_{7,8}$ ), left and right posterior superior iliac  
111 spines ( $T_{9,10}$ ), xyphoid ( $T_{11}$ ), manubrium ( $T_{12}$ ), first thoracic vertebra ( $T_{13}$ ),  
112 a rigid tripod fixed on the acromion ( $T_{14-16}$ ), under the deltoid ( $T_{17}$ ), medial  
113 side of the elbow ( $T_{18}$ ), olecranon ( $T_{19}$ ), and lateral and medial wrist ( $T_{20,21}$ ).  
114 One additional marker was placed at the middle of the bar ( $T_{22}$ ) between the  
115 hands. Markers  $T_{14-16}$  were removed before the data collection for the circling  
116 movements.

117 The dimensions of the model and the marker locations with respect to (*wrt*)  
118 the local segment reference frame had to be determined accurately. These  
119 required the determination of the centre of rotation (CoR) location and the

120 definition of the local frame associated with each body segment. Predictive  
 121 and functional approaches were used involving static and dynamic data ac-  
 122 quisition. The glenohumeral and hip CoR (modelled as ball and socket) were  
 123 located with the symmetrical CoR estimation method (Ehrig et al., 2006)  
 124 in line with the recommendation of Begon et al. (2007) and Monnet et al.  
 125 (in press) from markers  $T_{14-19}$  and  $T_{3-10}$  respectively. The pelvis local frame  
 126 was calculated from four markers ( $T_{7-10}$ ) using an optimisation procedure  
 127 (Challis, 1995). The elbow, wrist, knee, and ankle CoR (modelled as hinge  
 128 joints) were determined as the midpoint of lateral and medial markers. The  
 129 torso CoR relative to the pelvis was defined according to the anthropometri-  
 130 cal model of Yeadon (1990). Then the parameters were personalised for the  
 131 gymnast from the CoR locations during a static trial in anatomical posture.  
 132 Arm flexion causes elevation of the glenohumeral joint due to rotation about  
 133 the sternoclavicular joint. An initial position of the glenohumeral joint *wrt*  
 134 the torso frame was determined using the static trial data. From a trial with  
 135 arm flexion-extension motion, the scapular girdle elevation was modelled as  
 136 a linear function  $f$  of the arm flexion  $q_7$ . The location of each marker was  
 137 expressed in the local frame of the corresponding body segment and these  
 138 locations were introduced into the model.

139 From the data acquisition of stalders and endos on high bar, the generalized  
 140 coordinates ( $q_{1-12}$ ) were optimised for each frame. The resulting global op-  
 141 timisation was a non-linear programming problem so it had to be evaluated  
 142 numerically using iterative optimisation methods (a Newton-Gauss non-linear  
 143 least square algorithm). The reconstruction process was static; each posture  
 144 was determined independently from the one before. Ideally we would like to  
 145 obtain the generalized position vector  $\mathbf{q} = q_{1-12}$  such that:  $Tags(\mathbf{q}) = \mathbf{T}$ ,



where  $T_{ags}(\mathbf{q})$  is the forward kinematics function of the chain model and  $\mathbf{T} = T_{1-13,17-22}$  is the matrix of the observed marker positions. Based on the Jacobian of the  $T_{ags}$  ( $\partial T_i / \partial q_j$ ), the generalized co-ordinates were iteratively optimised in order to minimize  $\|T_{ags}(\mathbf{q}) - \mathbf{T}\|^2$ .

Three sets of kinematics were calculated using the chain model with, for each segment, three markers ( $Kin_{16}$ ):  $T_{1-7,9-13,19-22}$ , two markers ( $Kin_{11}$ ):  $T_{1,3,4,6,7,9,11,13,19,21,22}$  or only one marker except for the pelvis with two markers ( $Kin_7$ ):  $T_{1,4,7,9,11,19,22}$ .  $Kin_{16}$  was considered as the reference marker set. As skin deformation occurs in areas closer to the joints (Cappozzo et al., 1996), the markers used for  $Kin_{11}$  and  $Kin_7$  were chosen far from joints with large ranges of motion (shoulder, hip, back).

For each set of kinematics, the global error of reconstruction was defined by:

$$\frac{1}{M} \sum_{M=1}^M \frac{1}{F_m} \sum_{f=1}^{F_m} \sqrt{\frac{1}{3 \times N_{f,m}} \sum_{n=1}^{N_{f,m}} -12 \|T_{ags}(\mathbf{q}) - \mathbf{T}\|^2},$$

where  $M$  is the number of trials,  $F_m$  is the number of frames for trial  $m$  and  $N_{f,m}$  is the numbers of visible markers for frame  $f$  in trial  $m$ . The time histories of each generalized co-ordinate were compared by means of a root mean square difference (RMSD). RMSD of  $Kin_7$  and  $Kin_{11}$  relative to  $Kin_{16}$  were compared by means of a paired  $t$ -test ( $p < 0.05$ ).

### 3 Results

The reconstructions were processed in  $57 \pm 14$  ms,  $44 \pm 9$  ms and  $131 \pm 31$  ms for one frame of data and the global errors of reconstruction were  $26.7 \pm 3.0$  mm,  $26.7 \pm 3.4$  mm and  $31.4 \pm 2.5$  mm for  $Kin_{16}$ ,  $Kin_{11}$  and  $Kin_7$  respectively.

166 Whatever the trial, this error estimate decreased from  $Kin_{16}$  to  $Kin_{11}$  as  
167 well as from  $Kin_{11}$  to  $Kin_7$ . The marker occlusions varied from 0% to 65%  
168 of the total number of frames depending on the marker (Table 1). There  
169 were no occlusions for the markers  $T_{1,3,4,6,9,11,18,19,21,22}$ . The occlusion number  
170 of the other markers could reach half the frames ( $T_8$ ) or exceed it ( $T_{5,10}$ ).  
171 The occlusions of the markers fixed on the medial side of the lower left limb  
172 occurred when the legs were together, and the pelvis markers disappeared  
173 mainly during the piked posture. For  $Kin_7$  the markers were reconstructed in  
174 all the frames for the 20 movements except for the left anterior superior iliac  
175 spine  $T_7$  which had 22% occlusions ( $\pm 6\%$ ). Among the markers used for  $Kin_{11}$ ,  
176 the first thoracic vertebra marker  $T_{13}$  also had a few occlusions ( $4 \pm 7\%$ ).

177 [Table 1 about here.]

178 In general, the joint angles calculated from the three marker sets were similar  
179 (Fig. 3). The main differences were for the thigh mediolateral rotation ( $q_{11}$ )  
180 and the knee flexion ( $q_{12}$ ). The RMSD of the joint angles over the 20 circling  
181 movements ranged from  $1^\circ$  to  $39^\circ$  (Table 2). The RMSD of the arm rotation  
182 about the bar  $q_4$  for  $Kin_{11}$  and  $Kin_7$  relative to  $Kin_{16}$  never exceeded  $2.2^\circ$ .  
183 For  $Kin_{11}$  the maximum RMSD of the angles was less than  $13.0^\circ$  and the  
184 average RMSD was about  $3.7^\circ$ . The maximum values were found for the thigh  
185 mediolateral rotation ( $q_{11}$ ). For  $Kin_7$  this angle was imprecise with an average  
186 RMSD of  $39^\circ$  for a  $56^\circ$  range of motion. The other angles had an average  
187 difference of  $4^\circ$ . The RMSD of the prismatic joints ( $q_{5,6}$ ) remained less than  
188 6 mm for  $Kin_{11}$  and were in the order of a centimetre for  $Kin_7$ .

189 [Fig. 3 about here.]

190 [Table 2 about here.]

191 Only the RMSD of  $q_5$  (translation of the arm *wrt* the bar) did not change  
192 significantly ( $p = 0.49$ ) with the number of markers (Table 2). The other  
193 co-ordinates differed significantly ( $p < 0.001$ ); the RMSD values increased  
194 systematically with a reduction in marker number. On average, the RMSD  
195 values for  $Kin_7$  and  $Kin_{11}$  differed by less than  $4^\circ$  for  $q_{4,7,8,9,10,12}$  and by 9 mm  
196 for  $q_6$ . The main change was the thigh mediolateral rotation where the RMSD  
197 increased from  $10^\circ$  to  $39^\circ$  when  $T_{3,6}$  were removed in the change from  $Kin_{11}$   
198 to  $Kin_7$ .

## 199 4 Discussion

200 The purpose of this study was (*i*) to apply a global optimisation on a fast  
201 movement with large range of motion and (*ii*) to reduce the number of mark-  
202 ers for the kinematics reconstruction. A 9-parameter, 3-dimensional, 12-*DoF*  
203 chain model was shown to be suitable for modelling straddled movements on  
204 high bar and the kinematics reconstruction was precise with 11 markers or 7  
205 markers except for the thigh mediolateral rotation.

206 The proposed model seems to be a reasonable compromise between accuracy  
207 and simplicity of gymnast description for movements on high bar. The model  
208 was defined after observation, analyses and knowledge about circling move-  
209 ments on high bar (Hiley and Yeadon, 2003, 2005). On one hand, the kine-  
210 matics is constrained by the gymnastics rules (*i.e.* symmetrical movements,  
211 full extension of some joints); on the other hand the kinematics of the shoul-  
212 der is complex and the body length increases due to the high internal forces  
213 associated with the centripetal accelerations.

214 For simplicity of the model, the foot and head segments were considered to  
 215 be fixed *wrt* the shank and the torso respectively and the elbow was kept  
 216 fully extended. In gymnastics, the foot has to be aligned with the shank and  
 217 the lower-arm aligned with the upper-arm. The small amplitude of rotation  
 218 of these joints could have only a small effect on the dynamics. Simple ball  
 219 and socket or hinge joints do not model the real musculoskeletal system ac-  
 220 curately (Lu and O'Connor, 1999); joint models that are more anatomical  
 221 can be defined. The previous gymnast models for high bar movements (Hiley  
 222 and Yeadon, 2003, 2005) have been improved by introducing an extra *DoF* be-  
 223 tween the torso and the pelvis and by a personalised behaviour of the scapular  
 224 girdle elevation as a function of arm flexion ( $q_7$ ). The elevation of the scapular  
 225 girdle could not be estimated by the global optimisation procedure because it  
 226 would cause a singularity with  $q_6$  (arm lengthening) when  $q_7 = 0 \pm \pi$  (shoulder  
 227 flexion), *i.e.* if arm and trunk were aligned. The joint location in the back was  
 228 determined from observation of the whole spine flexion and according to the  
 229 anthropometrical model of Yeadon (1990). This chain model defined for me-  
 230 chanical analysis and optimisation of circling movement with piked straddled  
 231 postures has to be associated with an anthropometrical model to calculate the  
 232 kinetics.

233 The main experimental problem of straddled movements on high bar was the  
 234 marker occlusions. Despite using 18 cameras, there were a lot of occlusions for  
 235 the markers fixed on the medial side of the limbs ( $T_{2,4,18,20}$ ) or on the right  
 236 side of the pelvis ( $T_{8,10}$ ). The pelvis markers were also affected by the piked  
 237 posture. This explained 21% of occlusions for the left anterior superior iliac  
 238 spine marker  $T_7$ . A general placement of cameras cannot solve the problem  
 239 of occlusions since a specific placement for each athlete and each movement

240 is needed. Many athletic movement analyses would be impaired if at least  
241 three markers were required to define each segment, because marker occlusions  
242 could not be avoided and marker interpolation for movements involving high  
243 acceleration can result in kinematics with large errors. This approach based  
244 on a chain model compensates for marker occlusion.

245 The reference kinematics was chosen as the result of the global optimisation  
246 with 16 markers ( $Kin_{16}$ ) rather than the *direct approach* (Kadaba et al., 1990).  
247 In line with the works of Lu and O'Connor (1999) and Roux et al. (2002),  
248 global optimisation is more accurate than the *direct approach*. While these  
249 studies were based on computer simulated trials, the noise added to the marker  
250 kinematics was systematic (Chèze et al., 1995), this being more appropriate to  
251 model skin movement artefacts than random noise as confirmed by Begon et al.  
252 (2007). Furthermore in the present study, the direct method could be applied  
253 for only a few frames due to the marker occlusions throughout the movement  
254 (Table 1). The global optimisation works with any prior defined kinematic  
255 model structure and any experimental movement data without any restriction  
256 on the marker number and location while the Hessian remains of full rank.  
257 The *HuMAnS* toolbox (Wieber et al., 2006) allows new model chains to be  
258 implemented in order to reconstruct accurately the kinematics of movement  
259 with marker occlusions. The present algorithm will be improved in the future  
260 by introducing a weighting matrix in the Hessian and Jacobian expression and  
261 by a Kalman filter.

262 The precision of the kinematics obtained with the present algorithm was cal-  
263 culated for three sets of markers. The global error of reconstruction was about  
264 27 mm for  $Kin_{16}$  and  $Kin_{11}$ . The global error increased to 31 mm for  $Kin_7$ .  
265 The optimisation procedure always found a solution which depended on data

accuracy and redundancy. Using redundant information ( $Kin_{16}$  and  $Kin_{11}$ ), the chain model and markers compensated for each other's error. Since the error did not increase between  $Kin_{16}$  and  $Kin_{11}$ , the latter set of markers seemed to be a good compromise between the number of markers and their position to avoid skin movement artefacts. Global optimization provides a great opportunity to design optimal marker sets to minimize skin movement artefact, because less than three markers are needed on each body segment and the noisy markers can be removed.

The RMSDs found in this study for the thigh angles ( $q_{9-11}$ ) could be discussed in line with the errors measured using intra-cortical pins (Reinschmidt et al., 1997a,b; Karlsson and Lundberg, 1994). In running (Reinschmidt et al., 1997b) the errors expressed as a percentage of the range of motion were 21% for flexion-extension, 64% for abduction-adduction and 70% for mediolateral rotation of the thigh. These RMSDs during the circling movement with  $Kin_{11}$  on high bar corresponded to 2%, 1% and 18% of the thigh ranges of motion. For  $Kin_7$ , the RMSDs increased to 5%, 5% and 71%. Whatever the movement, the error associated with the mediolateral rotation of the thigh is the greatest. The study of Karlsson and Lundberg (1994) showed a difference of about  $30^\circ$  for the thigh mediolateral rotation calculated with skin-attached and bone-anchored markers ( $50^\circ$  *versus*  $20^\circ$ ). With global optimisation, the less noisy markers of pelvis and shank help to bring the thigh mediolateral rotation toward the correct orientation (Lu and O'Connor, 1999). The chain model and marker redundancy play an important role in compensating for errors. In this study, when the number of markers was reduced, the redundancy decreased and the inaccuracy increased. Since the knee was close to full extension, the mediolateral rotation ( $q_{11}$ ) was poorly compensated for by

the markers on the shank. The imprecision of  $q_{11}$  will have a small effect on the dynamics of straddled movements on high bar with straight legs. As the changes in knee flexion is small ( $\Delta q_{12} \approx 10^\circ$ ) and as the knee should be fully extended in gymnastics, some assumptions could be introduced into the chain model for a reconstruction with seven markers. The thigh mediolateral rotation and knee flexion could be assumed to be zero throughout the movement. An alternative would be to express  $q_{11}$  as a function of thigh flexion-extension and abduction-adduction.

In conclusion, kinematics can be reconstructed with a chain model and a global optimisation procedure for a reduced number of markers. The chain model makes the most of the information contained in all the markers. In the case of circling movements on high bar with a piked straddled posture, 11 markers allowed a 12-*DoF* model to be reconstructed within a  $3^\circ$ , 4 mm error. With the modifications suggested above it should be possible to obtain good results with 7 markers. Future studies will be based on the simplification of the model by expressing the trunk flexion and the thigh mediolateral rotation as functions of thigh flexion-extension and abduction-adduction.

## 5 Conflict of interest statement

There are no conflicts of interest to declare by the authors.

312 The authors wish to acknowledge the support of the British Gymnastics  
 313 World Class Programme and EGIDE (Ministère des Affaires Etrangères, France).

## 314 **References**

- 315 Begon, M., Monnet, T., Lacouture, P., 2007. Effects of movement for estimat-  
 316 ing the hip joint centre. *Gait & Posture* 25, 353–359.
- 317 Cappozzo, A., Catani, F., Leardini, A., Benedetti, M., Croce, U. D., 1996.  
 318 Position and orientation in space of bones during movement: experimental  
 319 artefacts. *Clinical Biomechanics* 11, 90–100.
- 320 Challis, J. H., 1995. A procedure for determining rigid body transformation  
 321 parameters. *Journal of Biomechanics* 28, 733–737.
- 322 Charlton, I. W., Tate, P., Smyth, P., Roren, L., 2004. Repeatability of an  
 323 optimised lower body model. *Gait & Posture* 20, 213–221.
- 324 Chèze, L., Fregly, B. J., Dimnet, J., 1995. A solidification procedure to facili-  
 325 tate kinematic analyses based on video system data. *Journal of Biomechan-*  
 326 *ics* 28, 879–884.
- 327 Davis, R., Ounpuu, S., Tyburski, D., Gage, J., 1991. A gait analysis data  
 328 collection and reduction technique. *Human Movement Science* 10, 575–587.
- 329 Ehrig, R. M., Taylor, W. R., Duda, G. N., Heller, M. O., 2006. A survey of  
 330 formal methods for determining the centre of rotation of ball joints. *Journal*  
 331 *of Biomechanics* 39, 2798–2809.
- 332 Hiley, M., Yeadon, M., 2003. Optimum technique for generating angular mo-  
 333 mentum in accelerated backward giant circles prior to a dismount. *Journal*  
 334 *of Applied Biomechanics* 19, 119–130.



335 Hiley, M., Yeadon, M., 2005. The margin for error when releasing the asym-  
 336 metric bars for dismounts. *Journal of Applied Biomechanics* 21, 223–235.

337 Kadaba, M., Ramakrishnan, H., Wootten, M., 1990. Measurement of lower  
 338 extremity kinematics during level walking. *Journal of Orthopaedic Research*  
 339 8, 383–392.

340 Karlsson, D., Lundberg, A., 1994. Accuracy estimation of kinematic data de-  
 341 rived from bone anchored external markers. In *Proceedings of the 3rd In-*  
 342 *ternational Symposium on 3-D Analysis of Human Motion.*

343 Lu, T.-W., O’Connor, J., 1999. Bone position estimation from skin marker  
 344 co-ordinates using global optimisation with joint constraints. *Journal of*  
 345 *Biomechanics* 32, 129–134.

346 Monnet, T., Desailly, E., Begon, M., Vallee, C., Lacouture, P., (in press) Com-  
 347 parison of the score and ha methods for locating in vivo the glenohumeral  
 348 joint centre. *Journal of Biomechanics.*

349 Reinbolt, J. A., Schutte, J. F., Fregly, B. J., Koh, B. I., Haftka, R. T., George,  
 350 A. D., Mitchell, K. H., 2005. Determination of patient-specific multi-joint  
 351 kinematic models through two-level optimization. *Journal of Biomechanics*  
 352 38, 621–626.

353 Reinschmidt, C., Bogert, A., Lundberg, A., Nigg, B., Murphy, N., Stacoff, A.,  
 354 Stano, A., 1997a. Tibiofemoral and tibiocalcaneal motion during walking:  
 355 external vs. skeletal markers. *Gait & Posture* 6, 98–109.

356 Reinschmidt, C., Bogert, A., Nigg, B., Lundberg, A., Murphy, N., 1997b. Ef-  
 357 fect of skin movement on the analysis of skeletal knee joint motion during  
 358 running. *Journal of Biomechanics* 30, 729–732.

359 Roux, E., Bouilland, S., Godillon-Maquinghen, A.-P., Bouttens, D., 2002.  
 360 Evaluation of the global optimisation method within the upper limb kine-  
 361 matics analysis. *Journal of Biomechanics* 35, 1279–1283.

- 362 Spoor, C., Veldpaus, F., 1980. Rigid body motion calculated from spatial  
363 coordinates markers. *Journal of Biomechanics* 13, 391–393.
- 364 Wieber, P.-B., Billet, F., Boissieux, L., Pissard-Gibollet, R., 2006. The hu-  
365 mans toolbox, a homogeneous framework for motion capture, analysis and  
366 simulation. In: *Ninth International Symposium on the 3D analysis of human*  
367 *movement*.
- 368 Yeadon, M. R., 1990. The simulation of aerial movement–II. A mathematical  
369 inertia model of the human body. *Journal of Biomechanics* 23, 67–74.

371	1	Model definition with the degrees of freedom and the	
372		parameters for the straddled circling movements on high	
373		bar. Degrees of freedom: $q_{1-3}$ translation of the bar, $q_4$ arm	
374		rotation, $q_5$ arm translation, $q_6$ arm lengthening, $q_7$ shoulder	
375		flexion, $q_8$ , spinal flexion, $q_9$ thigh flexion, $q_{10}$ thigh abduction,	
376		$q_{11}$ thigh lateral rotation and $q_{12}$ knee flexion. Parameters:	
377		$p_1$ arm length, $p_2$ torso length, $p_3$ half-width of the pelvis, $p_4$	
378		pelvis height, $p_5$ knee adduction and $p_6$ thigh length.	19
379	2	Straddled stalder (a) and endo (b) on high bar.	20
380	3	Time histories of the generalized co-ordinates for an endo	
381		calculated with 16, 11 and 7 markers.	21

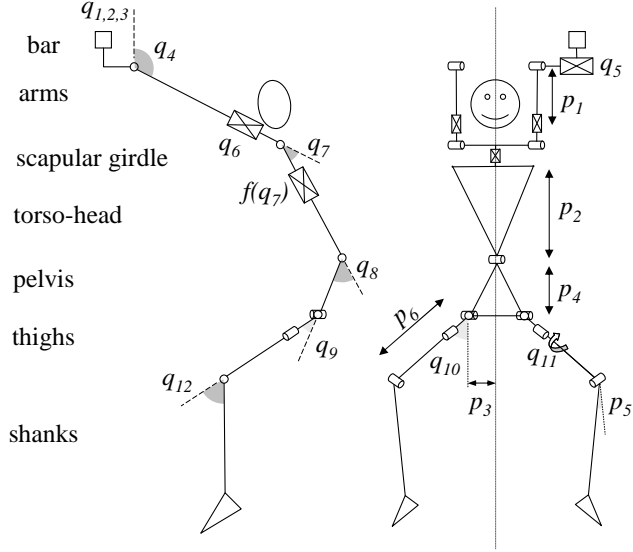


Fig. 1. Model definition with the degrees of freedom and the parameters for the straddled circling movements on high bar. Degrees of freedom:  $q_{1-3}$  translation of the bar,  $q_4$  arm rotation,  $q_5$  arm translation,  $q_6$  arm lengthening,  $q_7$  shoulder flexion,  $q_8$ , spinal flexion,  $q_9$  thigh flexion,  $q_{10}$  thigh abduction,  $q_{11}$  thigh lateral rotation and  $q_{12}$  knee flexion. Parameters:  $p_1$  arm length,  $p_2$  torso length,  $p_3$  half-width of the pelvis,  $p_4$  pelvis height,  $p_5$  knee adduction and  $p_6$  thigh length.

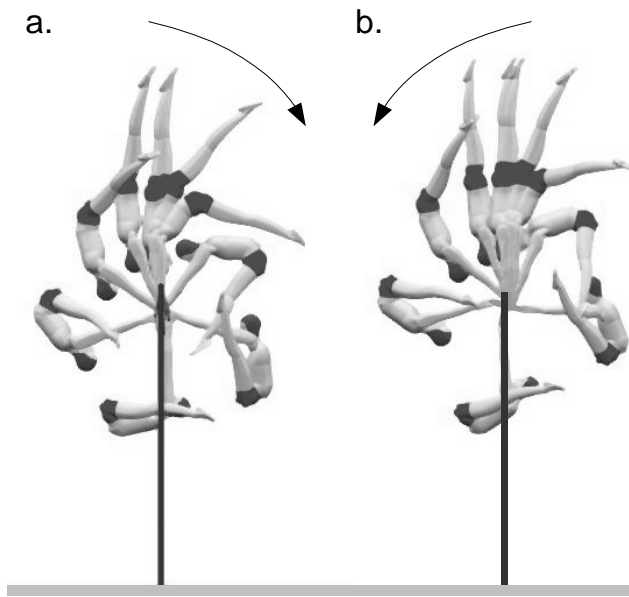


Fig. 2. Straddled stalder (a) and endo (b) on high bar.

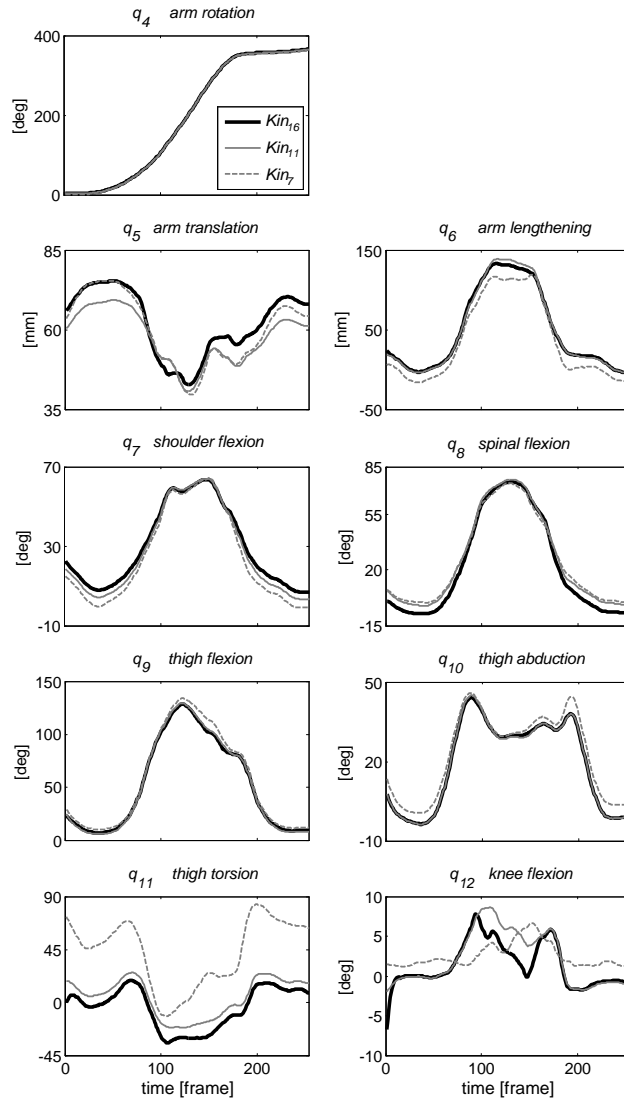


Fig. 3. Time histories of the generalized co-ordinates for an endo calculated with 16, 11 and 7 markers.

383	1	Marker occlusions during the circling movements	23
384	2	Root mean square difference for each global co-ordinate	
385		of $Kin_{11}$ and $Kin_7$ relative to $Kin_{16}$ , with notation	
386		$Kin_{11/16}$ , $Kin_{7/16}$ respectively	24

Table 1  
Marker occlusions during the circling movements

		mean	SD
Shank	$T_1$	0	(0)
	$T_2$	9	(17)
	$T_3$	0	(0)
Thigh	$T_4$	0	(0)
	$T_5$	65	(11)
	$T_6$	0	(0)
Pelvis	$T_7$	22	(6)
	$T_8$	42	(8)
	$T_9$	0	(0)
	$T_{10}$	56	(14)
Torso	$T_{11}$	0	(0)
	$T_{12}$	1	(2)
	$T_{13}$	4	(7)
Upper-limb	$T_{17}$	6	(6)
	$T_{18}$	0	(0)
	$T_{19}$	0	(0)
	$T_{20}$	6	(6)
	$T_{21}$	0	(0)
Bar	$T_{22}$	0	(0)

Note: the average values and the standard deviations are expressed as a percentage of the number of frames.



Table 2

Root mean square difference for each global co-ordinate of  $Kin_{11}$  and  $Kin_7$  relative to  $Kin_{16}$ , with notation  $Kin_{11/16}$ ,  $Kin_{7/16}$  respectively

	$q_i$	Unit	$Kin_{11/16}$	$Kin_{7/16}$	$p$	RoM
Arm Rotation	4	[°]	$0.5 \pm 0.1$	$1.3 \pm 0.3$	$< 0.001$	$457 \pm 154$
Arm Translation	5	[mm]	$4.1 \pm 1.2$	$4.4 \pm 1.9$	0.49	$33 \pm 7$
Arm Lengthening	6	[mm]	$3.3 \pm 0.6$	$12.3 \pm 2.6$	$< 0.001$	$158 \pm 18$
Shoulder Flexion	7	[°]	$2.1 \pm 0.5$	$4.9 \pm 1.0$	$< 0.001$	$64 \pm 11$
Spinal Flexion	8	[°]	$3.5 \pm 0.9$	$4.4 \pm 1.2$	$< 0.001$	$87 \pm 12$
Thigh Flexion	9	[°]	$2.0 \pm 0.5$	$6.0 \pm 1.7$	$< 0.001$	$131 \pm 9$
Thigh Abduction	10	[°]	$0.6 \pm 0.1$	$2.6 \pm 0.8$	$< 0.001$	$53 \pm 7$
Thigh torsion	11	[°]	$10.0 \pm 1.2$	$38.9 \pm 7$	$< 0.001$	$56 \pm 5$
Knee Flexion	12	[°]	$2.6 \pm 0.7$	$4.8 \pm 2.1$	$< 0.001$	$20 \pm 8$

Note: the fifth column is the  $p$ -value of the paired  $t$ -test between  $Kin_{11/16}$  and  $Kin_{7/16}$ . The last column is the range of motion (RoM) calculated with  $Kin_{16}$ .